Acta Cryst. (1975). A31, 101

Charge-Density Analyses for Molecular Crystals using Bragg Diffraction Data: the Effects of Error

BY A.J. ALLEN-WILLIAMS, W.T. DELANEY, R. FURINA, E.N. MASLEN. B.H. O'CONNOR, J.N. VARGHESE AND YUNG FOOK HONG

Department of Physics, University of Western Australia, Nedlands, Western Australia

(*Recevied* 5 *July* 1974; *accepted* 25 *July* 1974)

Charge-density analyses have been carried out on twelve sets of X-ray data. For materials containing first-row atoms intensities measured by the $\theta:2\theta$ method yield gross populations concordant with electronegativities and the shapes of the distributions agree qualitatively with predicitions from force-field arguments. Gross charges are sensitive to experimental errors systematic with Bragg angle, but are insensitive to deficiencies in the models for thermal motion. Noise in thermal parameters is a limiting factor for hydrogen populations determined from X-ray data alone, but mechanistic models for the hydrogen motions obviate this difficulty. Spherically symmetric functions centred at the nuclei give a poor representation of the density for bonded hydrogen. Slater-type orbital products with standard molecular exponents sample the valence density less efficiently for second-row atoms than for carbon, nitrogen and oxygen atoms. Two-centre density functions overlap heavily with neighbouring one-centre terms, and do not provide a useful extension to basis sets for charge-density studies. There are discrepancies between experimental populations and semi-empirical INDO calculations for strongly polar systems.

Introduction

In an idealized Bragg experiment the scattering amplitudes are the Fourier coefficients of the one-electron density function. The orders which can be measured are limited but the valence-electron contribution is maximal for the low-order Fourier coefficients, which are readily observed. In favourable cases, such as the 222 reflexion of diamond (Dawson, 1967*b*), other contributions to the scattering are negligible. More generally the effects of chemical bonding are small (Lipscomb, 1972), and the information which can be derived is limited by the range and quality of the intensity data, by the models used for deconvoluting the one-electron density function, and by the reliability of information on the departures from an idealized scattering experiment, such as dispersion and extinction.

For the molecular crystals with which this work is concerned the pioneering studies were those of McWeeny (1952, 1954). Important developments were made by Dawson (1967*a*). Stewart (1969) proposed that the electron density be expressed in terms of orbital products, and Coppens, Csonka & Willoughby (1970) have applied this to a range of problems. A difficulty arises in this approach because the Fourier components for products of different orbitals resemble one another within the range of the accessible data (Stewart, 1972). For example a one-centre $(2s)^2$ product has the same symmetry as a sum of $(2p_x)^2$, $(2p_y)^2$ and $(2p_z)^2$ products in equal proportions. The correspondence is exact for functions with the same radial dependence. The population coefficients for such products are strongly correlated, and are thus ill-defined.

The use of bond-directed scattering factors (O'Connor & Maslen, 1974) alleviates this problem. The shape of the density distribution is assumed to be consistent with nearest-neighbour geometry and bond hybridization. With each chemical bond, π bonds included, is associated a normalized density function $(\chi_s+\mu\chi_p)^2/(1+\mu^2)$. The hybridization ratio μ is $1, \sqrt{2}, \sqrt{3}$ and ∞ for approximate sp, sp^2, sp^3 hybridization and π bonding respectively. It is assumed that the two-centre terms, which are neglected, project into the one-centre terms with high efficiency. A projection analysis carried out by Stewart (1973*a*) justifies this assumption.

The optimum choice of radial variation for the density basis functions is still by no means clear. Theoretical calculations, such as those by Clementi (1967) indicate that the $1s^2$ core of first-row atoms is almost invariant to chemical bonding. This neglects core polarization, but this is a small, localized phenomenon affecting primarily high-order Fourier coefficients inaccessible to most X-ray diffraction experiments (Bentley & Stewart, 1974). Sets of self-consistent-field (SCF) wave functions for atomic $1s^2$ cores are included in tables by Clementi (1965).

The valence density for molecular systems has been written in terms of atomic SCF, single-term Slater-type orbital (STO) and other functions. The radial dependence of the valence density changes appreciably on bonding, and the results of charge-density analyses using atomic SCF functions have not been encouraging. STO functions have the virtue of simplicity, and their shapes can be varied by changing the exponent of the function. This can be determined from a scattering experiment, and Stewart (1973*b*) reports promising results for diamond, but for larger systems the calculations are less accurate and more expensive. Conse-

quently we have preferred the energy-optimized standard molecular exponents of Hehre, Stewart & Pople (1969). The main difference between the atomic SCF and Slater 2*s* functions is that the former have a cusp at the origin which is necessary to satisfy the condition that, for the electron density ϱ at the nucleus,

$$\left(\frac{\partial \varrho}{\partial r}\Big/\varrho\right)_{r=0} = -2Z$$

where Z is the nuclear charge. Stewart (1973*c*) has shown that neglect of the cusp produces an error in the temperature factor for diamond, but this is significant only for structures with low B values, and may be neglected for molecular crystals at room temperature.

Because of deficiencies in the sampling functions and experimental error, experimental integrated electron densities will not be equal to the correct values in general. Coppens, Pautler & Griffin (1971) avoid this problem by constraining the density model to preserve electrical neutrality. We prefer to use the projection efficiency as a measure of reliability, converting the populations to a neutral system by simply rescaling the populations as a last stage in the analysis.

Selection of data

Stewart (1970) considered the effects of experimental error on charge-density studies and concludes that estimation of gross electron populations is feasible with accurate data. His predictions are verified by the results of Stewart (1970), of Coppens, Pautler & Griffin (1971) and of O'Connor & Maslen (1974) who obtained atomic charges comparable with those from theoretical calculations for first-row atoms.

The aim of this study is to assess the viability of charge-density work as a general-purpose tool. This depends on its tolerance to experimental error, since collection of high-quality data is not feasible in every case of interest. We have therefore analysed the charge density in a variety of structures using data sets from different laboratories. These differ both in quality and in the range of reciprocal space which they span. In a number of cases the original authors did not have charge density work in mind when the data were collected.

Nevertheless some sets of data which were claimed to be accurate were rejected by us as unsatisfactory, on the basis of agreement analyses. In several cases the observed intensity I_o invariably exceeded the calculated intensity I_c for low I_o, indicating that either the background was underestimated or the weaker intensities were set equal to a multiple of the standard deviation without note of this in tables or text. Data sets from one laboratory had an abrupt discontinuity in the I_o/I_c ratio in the high I_o range, probably resulting from an incorrectly calibrated attenuator. In trial refinements with these discordant sets the gross electron populations for chemically equivalent atoms differed by several standard deviations, and bore little relation to the electronegativities of the atoms involved.

Not all the data considered below are free from systematic error, but the errors are primarily a property of the data-collection technique. The cases are instructive and warrant examination.

Oxalates and related compounds

The oxalates have been studied extensively and are suitable for a series of charge-density analyses on related polar materials. Details of the data sets available are given in Table 1.

Oxalic acid dihydrate

Neutron diffraction data is available for this material and the X-ray set is accurate, but not extensive. The charge density, first studied quantitatively by Coppens, Pautler & Griffin (1971), serves as a standard for the series. The data were re-analysed using bond-directed scattering factors. Population coefficients were determined for $(sp^2)^2$ products for carbon and oxygen in the oxalate ion, $(sp^3)^2$ products for the water oxygen and $(1s)^2$ products for hydrogen with the structural parameters taken from the neutron analysis. The residual was based on $|\mathbf{F}|^2$. Subsequently they were redetermined using the original X-ray parameters. The results are given, along with those of Coppens, Pautler & Griffin (1971) and the gross Mulliken populations for a semi-empirical INDO calculation (Pople & Beveridge, 1970), with two water molecules situated as in the crystal structure, in Table 2. For comparison purposes similar populations are given for an INDO calculation on a neutral oxalate radical and for a Hückel-type calculation on the same radical with an excess of one electron.

One aspect of the results is worthy of special note. The populations of the hydrogen atoms are about 0·15 e higher when the sampling functions are centred on

Table 1. *Details of data sets for oxalates and related compounds*

Structure	Space group	Data	$\sin\theta_{max}/\lambda$	Author & reference
α-Oxalic acid dihydrate	$P2_1/n$	544 Cu $K\alpha$ X-ray + neutron	0·53	Delaplane & Ibers (1968) Sabine, Cox & Craven (1969)
Potassium oxalate monohydrate	$P2_1/c$	1153 Mo $K\alpha$ X-ray + neutron	0·86	Hodgson & Ibers (1969) Sequeira, Srikanta & Chidambaram (1970)
Lithium oxalate	$P2_1/n$	345 Cu $K\alpha$ X-ray	0·64	Beagley & Small (1964)
Ammonium oxamate	$P2_1/n$	937 Cu $K\alpha$ X-ray	0·64	Beagley & Small (1963)
Acetohydroxamic acid hemihydrate	$Pnn2$	453 Cu $K\alpha$ X-ray	0·63	Bracher & Small (1970)

the X-ray positions, which correspond to the condition of maximum overlap between the observed density and the model. When the sampling function is centred on the position from the neutron analysis the drop in sampling efficiency is pronounced. This also spuriously enhances the population of the neighbouring oxygen, exaggerating the degree of polarity. Apart from this the experimental results span the theoretical values for the structure.

The density around the carbon and oxygen nuclei is consistent with force-field arguments based on static Coulomb interactions with the nearest-neighbour atoms. The local dipole at the carbon atom arises from a higher electron density in the C–C direction than along the C=O bonds, counteracting the effect of the charge on the neighbouring carbon and oxygen atoms. Likewise the local dipole at the oxygen atom O(2), resulting from the density being higher in the O–C direction than towards the lone pairs, opposes the force due to the positive charge on the neighbouring carbon, and the density for the water oxygen directed along the O–H bonds exceeds that directed towards the lone pairs.

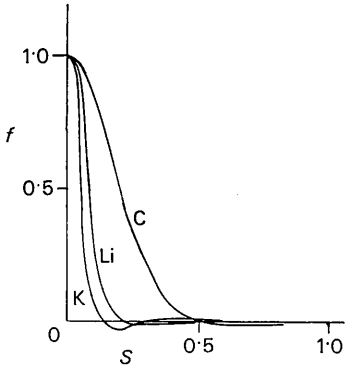

Fig. 1. Radial dependence of valence scattering amplitudes per electron for carbon, lithium and potassium. The carbon and lithium curves are calculated using Slater-type orbitals with standard molecular exponents. The potassium curve is the difference between the free-atom and free-ion form factors. ($S=\sin\theta/\lambda$).

Potassium oxalate monohydrate

In this analysis the valence scattering is a smaller fraction of the total than in oxalic acid, and lower accuracy is expected. There are two additional problems. The dominance of the potassium-ion scattering limits the precision of the X-ray parameters for the other atoms, and especially for the hydrogen. Consequently all the calculations were carried out using neutron parameters. Secondly the nature of the density associated with the potassium ion is less well established than those for first-row atoms.

For the oxalate ion and water molecule bond-directed scattering factors were calculated as for oxalic acid. The valence scattering for the potassium was assumed to be spherically symmetric, with a magnitude equal to the difference between the free atom and a core consisting of the free ion, using the scattering factors in *International Tables for X-ray Crystallography* (1962). This difference is illustrated in Fig. 1. Valence scattering factors for carbon and lithium are included for comparison. The potassium valence scattering for the shortest non-zero reciprocal-lattice vector in this structure is less than 0·07 e, and it exceeds 0·03 e for only seven reflexions. The measurement of its charge is less precise than those for the first-row atoms.

Table 2. *Bond-directed scattering-factor refinements for oxalic acid dihydrate*

Bond-directed and total valence populations ($e\times10^2$), rescaled to give a neutral molecule with projection coefficient ($\times10^2$) and refinement indices ($\times10^3$). P_1, P_2 and P_3 are parallel to the C(1)–C(1′), C(1)–O(1) and C(1)–O(2) bonds for C(1) and antiparallel to these for O(1) and O(2). P_1, P_2, P_3 and P_4 are parallel to O(3)–H(2), O(3)–H(3) and the two tetrahedrally related directions respectively. P_c is the total valence population obtained by Coppens, Pautler & Griffin (1971), and P_{t1}, P_{t2} and P_{t3} the gross Mulliken populations from an INDO calculation for oxalic acid plus water, a neutral oxalate radical, and a Hückel-type calculation for a $(COO)_2^-$ radical. The upper and lower figures correspond to refinements using neutron and X-ray parameters respectively.

	P_1	P_2	P_3	P_4	P_π	P_{val}	P_c	P_{t1}	P_{t2}	P_{t3}
C(1)	113 (8)	107 (10)	73 (11)		52 (13)	346 (16)	378 (5)	357	348	383
	93 (6)	67 (8)	36 (9)		108 (10)	304 (13)				
O(1)	166 (9)	204 (9)	182 (8)		112 (14)	663 (12)	636 (5)	628	626	658
	183 (7)	200 (7)	174 (7)		102 (11)	658 (11)				
O(2)	126 (8)	220 (9)	224 (10)		84 (15)	654 (15)	632 (4)	633	626	658
	153 (6)	162 (7)	207 (8)		135 (12)	657 (11)				
O(3)	190 (10)	201 (10)	146 (9)	112 (9)		649 (16)	643 (5)	632		
	203 (8)	195 (8)	135 (7)	115 (8)		647 (11)				
H(1)						79 (10)	71 (2)	81		
						94 (8)				
H(2)						70 (10)	78 (2)	84		
						83 (9)				
H(3)						40 (12)	63 (2)	84		
						55 (9)				

Projection coefficient	R		
	ωF^2	F^2	F
92	187	112	82
78	135	75	59

A further difficulty arises because of dispersion. The X-ray data were collected using Mo $K\alpha$ radiation, and dispersion is appreciable only for the potassium ion. Measurements of the change in scattering with wavelength appear to confirm the validity of the theoretical values (Persson & Grimwall, 1970), but Roof (1967) reports experimental measurements of $\Delta f'$ which are consistently more negative than indicated by theory. The results might be reconciled if the 'atomic' cores in the solid are a shade more diffuse than in the free atom. This is reasonable on energetic grounds, but precise calculations are difficult and the effective dispersion scattering factor is therefore uncertain.

The bias in a valence population due to an error in dispersion was investigated analytically. It is small as long as the valence scattering is large compared with dispersion for some reflexions, but interaction between valence populations and errors in the dispersion term will be appreciable for cases such as the potassium in this structure. This was verified by conducting two refinements, one using the dispersion scattering amplitudes given in *International Tables for X-ray Crystallography* (1962) and the other treating these as variable parameters.

The results of the refinements are given in Table 3. There are no significant differences between the two refinements. The refined dispersion terms do not differ significantly from the theoretical values, but the real component is more negative, in accordance with the results of Roof (1967).

Table 3. *Bond-directed scattering-factor refinements for potassium oxalate monohydrate*

Bond-directed and total valence populations ($e \times 10^2$) with projection coefficients ($\times 10^2$) and refinement indices ($\times 10^3$). Bond directions are similar to those for Table 2. The first and second figures are results with fixed and variable dispersion terms respectively. The component values and P_{val1} are those with the oxalate group and the water molecule scaled to 20 e. P_{val2} are the same gross populations scaled to 21 e.

	P_1	P_2	P_3	P_π	P_{val1}	P_{val2}
C(1)	130 (7)	115 (9)	110 (10)	40 (10)	394 (14)	414 (15)
	122 (8)	123 (9)	116 (10)	38 (10)	400 (14)	420 (15)
O(1)	170 (7)	150 (7)	167 (7)	141 (9)	627 (9)	658 (10)
	161 (7)	157 (7)	168 (7)	136 (9)	622 (10)	653 (11)
O(2)	173 (6)	157 (7)	143 (8)	138 (9)	611 (9)	641 (10)
	161 (6)	158 (7)	144 (8)	140 (9)	604 (10)	634 (11)
O(3)	158 (7)		144 (6)		604 (14)	634 (15)
	159 (7)		143 (6)		603 (14)	633 (15)
H					66 (11)	70 (11)
					74 (11)	78 (11)
K^+					106 (180)	
					215 (169)	
$\Delta f'(K^+)$					21	
					−11 (5)	
$\Delta f''(K^+)$					30	
					92 (15)	

Projection coefficient	R ωF^2	F^2	F
98	71	97	52
93	53	96	50

The valence population for the potassium is expected to lie between 0·0 and 1·0, while the experimental values are 1·1 (1·8) and 2·2 (1·7) e for the two refinements. No useful information has been obtained. The direct effect of dispersion is important only for the potassium, but the uncertainty has an indirect effect on the remaining populations *via* the rescaling factor. The results in Table 3 were calculated using the expected extremes, rather than the experimental values, for the potassium shell.

The carboxyl group appears to be less polar than the theoretical calculations or the corresponding group in oxalic acid. The population of the water hydrogen is rather low, confirming the effect of poor overlap between experimental and model densities for hydrogen when the latter is placed at the proton positions.

The distribution of density around the carbon and the oxygen is similar to that in oxalic acid, but for the carboxyl oxygens the results are contradictory, since the electron density in the direction of the C=O bonds is a minimum in this structure. This might be dismissed as an artefact resulting from lower accuracy, but contradictory results have also been obtained from other sets of data (Epstein, 1972). The problem may be related to deficiencies in the treatment of the thermal motion which are more serious for atoms in terminal positions, but definitive work on this point is not available.

Lithium oxalate

In lithium oxalate the valence density contributes a higher proportion to the total scattering. The small cell size restricts sampling in the low-angle region but the valence scattering for lithium is more extensive than for the other alkali metals. A moderately reliable measurement of its population was expected.

The high absorption cross section of normal lithium is a deterrent to neutron diffraction experiments and no suitable neutron data is available. The X-ray data set had been collected using Cu $K\alpha$ radiation, and dispersion may be appreciable. There is also some evidence for extinction in this data, which offers an opportunity for studying the effects of extinction and dispersion on the population coefficients. Notwithstanding reservations regarding the physical interpretation of its parameters (Killean, Lawrence & Sharma, 1972), the expressions of Zachariasen (1967) appear to provide a satisfactory treatment of extinction when the corrections are small. Accurate corrections are impossible in the present case, since information on the crystal shape is unavailable, but an analytical investigation indicated that interaction between the extinction parameter and the valence populations would be small. The extinction factor depends on the product $r^*\bar{T}$, where r^* is a modified domain radius and $\bar{T}$ is the mean path length for the radiation in the crystal. The scale of $\bar{T}$ is unimportant if r^* is to be determined only to within a factor. A constant value for $\bar{T}$ of 0·1 mm was used as a reasonable approximation.

Correlation between the dispersion corrections and the valence populations was expected to be small, and only the largest dispersion term, *i.e.* the anomalous scattering for oxygen, was considered. The electron-density model was similar to that used for potassium oxalate monohydrate, except that the valence contribution for lithium was constructed from a $(2s)^2$ STO product with standard molecular exponent. Three refinements were carried out. In the first the scale, positional, thermal and population parameters were varied, while extinction and dispersion were omitted. The second included extinction and dispersion with the scattering amplitude given in *International Tables for X-ray Crystallography* (1962). In the third the dispersion amplitudes for both oxygens were refined independently. Extinction was introduced at a late stage in these analyses and produced virtually no change in the population parameters.

The pertinent results from these refinements are given in Table 4. The valence-shell population for the lithium is zero within the error, but partial occupancy is not excluded by the standard deviations. The population was treated as zero for the purpose of rescaling. The oxalate group is more strongly polar than that in the potassium oxalate monohydrate analysis. This is consistent with the trend observed in oxalic acid where the use of X-ray parameters appears to produce a more polar structure. In all three analyses the in-plane populations for the oxygen atoms are higher than the P_π populations. This is most marked where X-ray parameters were used, and it seems that variation of the thermal parameters has resulted in too high a fraction of the σ charge being associated with the oxygen atoms. The local dipoles at the carbon and oxygen atoms are similar to those in oxalic acid.

Ammonium oxamate

The analysis of ammonium oxamate permits a study of the ammonium ion, but without neutron data the thermal parameters for hydrogen are poorly defined. In the original structure determination Beagley & Small (1963) treated the thermal motion as isotropic. This gives a determination of higher precision than an anisotropic analysis, but neglect of anisotropy will be similar in its effect to the use of a model density function with an exponent which varies with orientation. This is undesirable, and it was decided to treat the thermal motion for all the atoms as anisotropic.

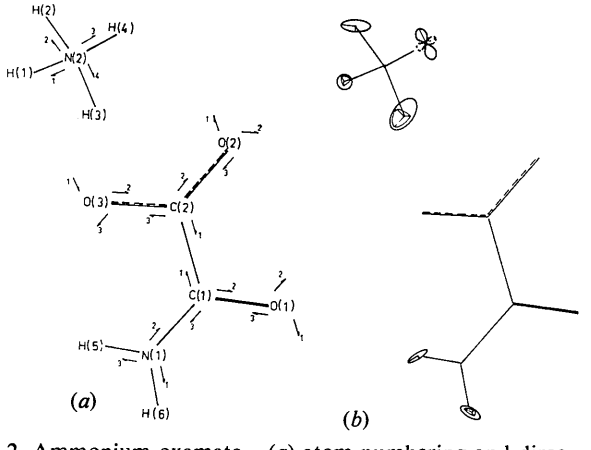

Fig. 2. Ammonium oxamate – (*a*) atom numbering and directions for bond-directed scattering factors (*b*) thermal ellipsoid r.m.s. amplitudes for the hydrogen atoms. The broken line indicates an imaginary eigenvalue for H(4).

Table 4. *Bond-directed scattering-factor refinements for lithium oxalate*

Bond-directed and total valence populations ($e \times 10^2$) with domain radius (cm $\times 10^6$), projection coefficients ($\times 10^2$) and refinement indices ($\times 10^3$). Bond directions are similar to those for Table 1.

	P_1	P_2	P_3	P_π	P_{val}	$\Delta f''$
C(1)	130 (9)	72 (16)	61 (16)	82 (17)	345 (21)	
	131 (9)	68 (17)	64 (17)	79 (17)	341 (21)	
	131 (9)	68 (16)	64 (16)	79 (17)	342 (21)	
O(1)	180 (16)	211 (21)	167 (16)	119 (29)	677 (22)	0
	193 (17)	235 (20)	177 (16)	77 (27)	681 (21)	18
	192 (16)	234 (20)	177 (16)	78(27)	681 (21)	8 (19)
O(2)	203 (18)	184 (16)	228 (20)	63 (27)	678 (21)	0
	204 (19)	178 (15)	221 (20)	74 (20)	677 (21)	18
	204 (18)	180 (15)	222 (20)	71 (27)	677 (21)	15 (17)
Li^+					−3 (100)	
					−15 (107)	
					−17 (106)	

r^*	Projection coefficient	R ωF^2	F^2	F
0	87	207	101	56
32 (59)	85	205	96	57
32 (59)	85	204	94	55

The electron-density model was consistent with the preceding studies. The vectors specifying the bond-directed scattering factors are shown in Fig. 2(*a*). Anomalous-dispersion scattering factors for oxygen and an extinction factor were included as variables, and the populations were again insensitive to these terms. It was necessary to use an arbitrary constant value of $\bar{T}$ equal to 0·1 mm as an approximation. As the shifts in the previous analyses had been negligible the atomic positions were not refined. The core memory needed for full-matrix refinement exceeded that available, so the matrix was positioned into blocks, one for each atom in the structure, with another for the scale factor and extinction.

Results of the refinement are given in Table 5. The anomalous-dispersion terms for the oxygen atoms agree remarkably well with each other. They are also in accord with the values obtained in the lithium oxalate analysis, and they do not differ significantly from the theoretical value. Qualitatively the populations for the carbon, nitrogen and oxygen atoms are satisfactory since the carbons alone have electron deficiencies. The positive charge on the carboxyl carbon is rather large, and ideally the negative charges on the carboxyl oxygens O(1) and O(2), the amide oxygen O(3) and the amide nitrogen N(1) should decrease in that order, but it was not expected that precise values

would be obtained with this data. The nitrogen atom N(2) in the ammonium ion is negatively charged. This conflicts with the observation of McDonald (1960) on the ammonium ion in hydrogen fluoride, but that was based on the assumption that density functions from the unbound state are appropriate for sampling bonded density. The subdivision of charge between bound atoms is to some extent arbitrary and depends on the sampling functions used to assess this charge. Because lower energies are obtained with the use of contracted orbitals in variational calculations, optimized exponents appear to be more appropriate for molecular systems. The present result is also more reasonable in view of the electronegativities of the atoms involved.

Table 5. *Bond-directed scattering-factor refinement for ammonium oxamate*

Bond-directed and total valence populations ($e \times 10^2$), with domain radius, ($cm \times 10^6$) projection coefficients ($\times 10^2$) and refinement indices ($\times 10^3$). The vector directions associated with the scattering factors are indicated in Fig. 2(*a*).

	P_1	P_2	P_3	P_4	P_π	P_{val}	$\Delta f''$
C(1)	114 (5)	97 (5)	100 (5)		69 (8)	379 (5)	
C(2)	113 (5)	94 (5)	93 (5)		41 (8)	341 (5)	
N(1)	106 (5)	113 (5)	101 (5)		188 (11)	508 (4)	
N(2)	115 (4)	139 (4)	133 (4)	133 (4)		521 (6)	
O(1)	143 (5)	161 (5)	163 (5)		151 (14)	618 (4)	14 (6)
O(2)	148 (5)	155 (6)	148 (5)		155 (14)	606 (4)	17 (6)
O(3)	141 (6)	165 (6)	161 (6)		143 (14)	611 (4)	16 (6)
H(1)						84 (5)	
H(2)						101 (4)	
H(3)						129 (6)	
H(4)						64 (4)	
H(5)						111 (4)	
H(6)						127 (6)	

	Projection	R		
r^*	coefficient	ωF^2	F^2	F
450 (163)	91	132	71	41

The shapes of the distributions around the carbon and oxygen nuclei are consistent with force-field arguments, and the mean P_π population for the oxygen atoms is lower than the mean of the in-plane components, but only marginally so. The high errors in the P_π populations results from poor sampling in the direction normal to the molecular plane.

Although the results for the carbon, nitrogen and oxygen atoms are consistent there are anomalies in the populations for the hydrogen atoms. Those in the ammonium ion appear to differ significantly in a manner which is not related to structure. The amino hydrogens are involved in N–H···O hydrogen bonds, but appear to be negatively charged, which is wildly improbable. The standard deviations, which come from the diagonal elements of the inverse matrix, are clearly unreliable for these atoms and it is necessary to look for an additional source of error in the parameters. Thermal ellipsoids for these hydrogen atoms are shown in Fig. 2(*b*). There is an obvious correlation between the

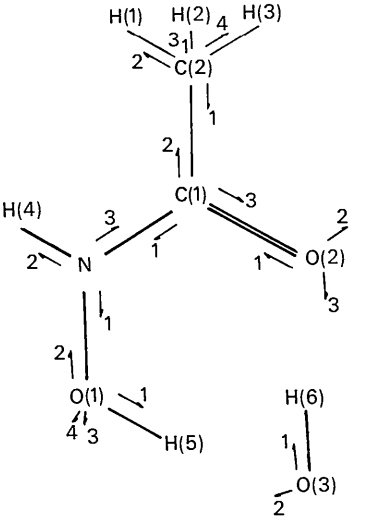

Fig. 3. Acetohydroxamic acid hemihydrate – atom numbering and directions for bond-directed scattering factors.

Table 6. *Bond-directed scattering-factor refinement for acetohydroxamic acid hemihydrate*

Bond-directed and total valence populations ($e \times 10^2$), with domain radius ($cm \times 10^6$), projection coefficient ($\times 10^2$) and refinement indices ($\times 10^3$). The vector directions associated with the scattering factors are indicated in Fig. 3.

	P_1	P_2	P_3	P_4	P_π	P_{val}	$\Delta f''$
C(1)	102 (11)	101 (12)	127 (13)		42 (21)	372 (12)	
C(2)	123 (12)	135 (18)	50 (25)	110 (15)		418 (13)	
N	141 (12)	145 (13)	159 (12)		36 (25)	481 (11)	
O(1)	136 (16)	147 (9)	147 (11)	193 (21)		623 (10)	−22 (8)
O(2)	180 (14)	165 (12)	174 (12)		93 (29)		−4 (5)
O(3)	149 (20)		144 (19)			586 (14)	1 (7)
H(1)						80 (13)	
H(2)						44 (9)	
H(3)						91 (13)	
H(4)						139 (16)	
H(5)						79 (13)	
H(6)						167 (16)	

	Projection	R		
r^*	efficiency	ωF^2	F^2	F
245 (121)	94	158	84	62

population coefficients and the thermal parameters. Too large thermal vibration has the effect of broadening the sampling function, increasing the population, and *vice-versa*.

In assessing the charge on the ammonium ion we prefer the weighted mean of the hydrogen populations to a simple average, obtaining a value of 0·89 e per hydrogen atom. Taking the difference between the populations of the ammonium-ion hydrogens as a guide to accuracy the net charge on the ammonium ion is 0·20 (52) e. The charge on the oxamate ion is −0·01 (37) e, which does not balance the ammonium charge because of the use of the weighted average. It is reasonably encouraging in view of the problem with the hydrogens that these lie between zero and one, as expected.

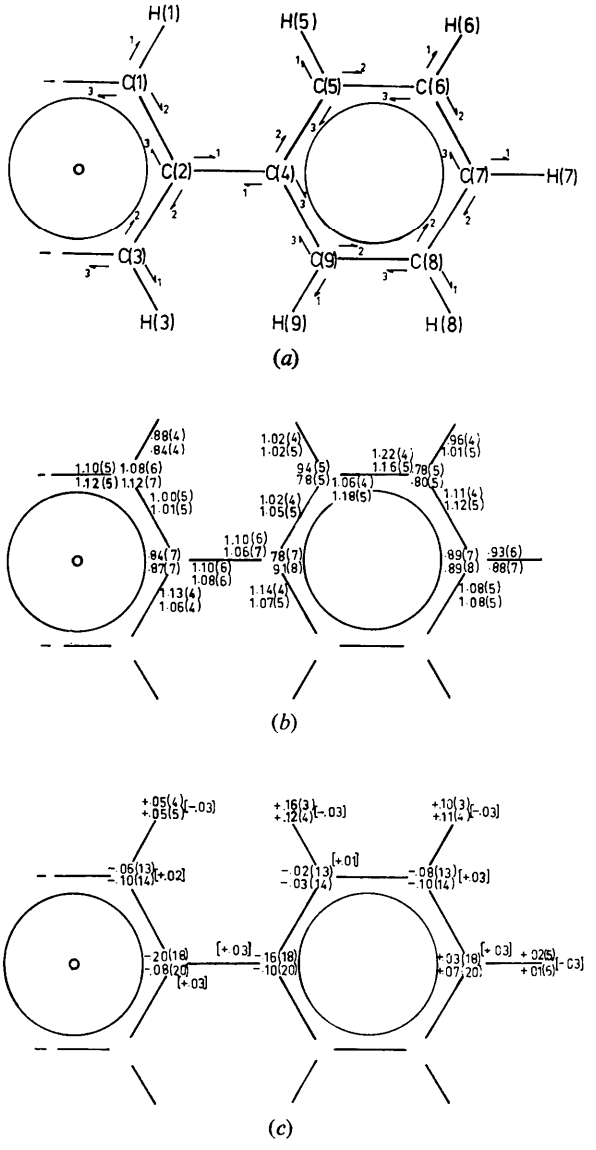

Fig. 4. *p*-Terphenyl – (*a*) atom numbering and directions for bond-directed scattering factors (*b*) component populations for carbon atoms and (*c*) net charges, in electrons, rescaled, with chemically equivalent values averaged. The upper and lower figures correspond to the mechanistic and statistical models respectively, with theoretical values in square brackets. Only the half molecule within the asymmetric unit of the structure is shown.

Acetohydroxamic acid hemihydrate

The structure and data set quality are similar to those of the preceding analysis, and the charge-density refinement followed the same procedure. The directions of the vectors used to define the electron-density model are shown in Fig. 3, and the results are given in Table 6.

The behaviour of the hydrogen populations confirms the results of the ammonium oxamate analysis. The thermal ellipsoids for atoms H(2), H(5), H(1) and H(3) have three, two, two and one imaginary eigenvalues respectively. Their populations increase in this order. H(4) and H(6) have over-large thermal parameters. Their populations are correspondingly high. In the latter case this has the effect of depressing the population for O(3), to which it is bonded. The standard deviations for all P_π populations, P_3 for C(2) and P_4 for O(1) are high, and the last two populations are obvious outliers in the results. The defining vectors for the corresponding density functions are almost parallel to the short axis of the cell in each case. This is a further example of the sampling problem which afflicts charge-density analysis when applied to small cells. It is generally responsible for the poor definition of the P_π populations in these oxalate structures, all of which have a short axis normal to the molecular plane.

Aromatic hydrocarbons

Previous charge-density analyses have been largely confined to polar materials with low temperature factors, for which high-angle data can be collected. However there is a clear advantage in studying a non-polar material to test the reliability of the technique. Van der Waals interactions between molecules are weaker than the interactions between static charges in polar systems. The perturbing effects on the electron density will be correspondingly reduced and a theoretical calculation for an isolated molecule should give a reasonable description of the charge density in the crystal.

The set of X-ray diffraction data collected by Robertson (1965) represents a serious attempt at accurate data collection. The measurements were repeated many times, involving some years of experimental work. However, thermal motion in this structure is large, and it was necessary to examine the effect of deficiencies in the model for thermal motion on charge-density studies before analysing the diphenyl data.

p-Terphenyl

p-Terphenyl, for which a structure refinement was reported by Rietveld, Maslen & Clews (1970) has

structural properties which are suitable for exploring any systematic relationship between the thermal model and the charge distribution. The thermal motion is dominated by hindered rotations of the rings about the long axis of the molecule. These are of unusually large amplitude. The material is an alternant hydrocarbon, for which charge movements between atoms are zero to first order (Coulson, 1961). The problem of differentiating errors in the thermal model from movements of charge due to chemical bonding is minimized.

Furina & Maslen (1975) have analysed the thermal motion using neutron diffraction data, in terms of models based on two different analytical techniques. In a statistical model parameters for a Gaussian thermal-smearing function were determined independently for each atom, whereas in a mechanistic model the thermal motion was treated as the resultant of a set of vibrational and librational modes, and the temperature factors included an allowance for curvature in the motion (Maslen, 1970).

A set of X-ray data was collected and details are given in Table 7. The crystal was taken from the batch prepared by Furina & Maslen (1974). Unfortunately it was not found possible to trim a specimen to X-ray size without disordering the crystal, and following Rietveld, Maslen & Clews (1970) this was allowed for by the inclusion of an artificial temperature factor for the structure as a whole. How well this represents the effects of distortion is uncertain, and it is possible that the data contains some residual systematic error. The model for the electron density was based on bond-directed scattering factors directed as in Fig. 4(*a*). Weights were taken from the counting statistics, modified for experimental error as suggested by Grant, Killean & Lawrence (1969) and Killean & Lawrence (1969).

Table 7. *X-ray data collection for p-terphenyl*

Monoclinic $a=8{\cdot}1075$ (13), $b=5{\cdot}6111$ (7), $c=13{\cdot}6086$ (16) Å
$\beta=92{\cdot}005$ (10)°
obtained from the 2θ measurements of reflexions using Cu $K\alpha_1$, and Cu $K\alpha_2$ radiation. λ(Cu $K\alpha_1$) = 1·54051, λ(Cu $K\alpha_2$) = 1·54433 Å

Crystal dimensions $0{\cdot}016\times0{\cdot}029\times0{\cdot}034$ cm. Data collection using hybrid construction automatic four-circle diffractometer with θ:2θ scan using Ni-filtered radiation, scan range 1·5–2·4°. Dead-time losses were not significant. The intensities were corrected for Lorentz and polarization factors, and for absorption by the method of the Meulenaer & Tompa (1965).

The results of the refinement are given in Table 8. If perturbations due to intermolecular forces are small corresponding populations for C(1), C(3), H(1), H(3), C(5), C(9), H(5), H(9), C(6), C(8), H(6), H(8), which are chemically equivalent in pairs, should be equal within the error. This is generally true. It is then valid to average the populations, reducing the effect of random error. These averages are given in Fig. 4(*b*), and the corresponding charges are given in Fig. 4(*c*). The gross populations for the statistical and mechanistic models differ very little. There are some significant changes in the shapes of the distributions around the nuclei. Even these are relatively small considering the large amplitudes of libration in this structure. The reliability of the thermal model is thus of limited importance in the analysis for the measurement of gross charges, but requires some attention in analyses of the shapes of the local distributions. This may account for some of the anomalous results obtained for terminal atoms (Epstein, 1972).

Table 8. *Bond-directed scattering-factor refinements for p-terphenyl*

Bond-directed and total valence populations ($e\times10^2$) rescaled to give a neutral molecule, with projection coefficient ($\times10^2$), refinement indices ($\times10^3$) and $\Delta\beta_{ij}$($\times10^5$). The upper and lower figures correspond to the mechanistic and statistical model in each case. The vector directions associated with the scattering factors are given in Fig. 3(*a*).

	P_1	P_2	P_3	P_π	P_{val}		P_{val}
C(1)	76 (6)	88 (7)	93 (7)	128 (9)	386 (18)	H(1)	99 (6)
	87 (7)	103 (7)	131 (8)	98 (10)	420 (20)		94 (7)
C(2)	110 (6)	112 (6)	114 (6)	84 (7)	420 (18)	H(3)	89 (6)
	108 (6)	115 (7)	97 (7)	87 (7)	408 (20)		96 (7)
C(3)	100 (6)	112 (7)	127 (7)	88 (9)	427 (18)	H(5)	79 (5)
	82 (7)	99 (8)	94 (8)	125 (10)	401 (20)		85 (6)
C(4)	110 (6)	116 (6)	112 (6)	78 (7)	416 (18)	H(6)	90 (5)
	106 (7)	108 (7)	106 (7)	91 (8)	410 (20)		94 (6)
C(5)	109 (6)	101 (6)	107 (6)	90 (8)	406 (18)	H(7)	98 (5)
	106 (7)	112 (7)	121 (7)	71 (8)	409 (20)		99 (6)
C(6)	107 (6)	115 (7)	117 (7)	70 (7)	409 (18)	H(8)	91 (6)
	116 (7)	111 (8)	100 (7)	73 (8)	400 (20)		84 (6)
C(7)	93 (6)	119 (7)	96 (7)	89 (7)	397 (18)	H(9)	90 (5)
	88 (7)	121 (7)	94 (8)	89 (8)	393 (20)		91 (6)
C(8)	85 (6)	107 (7)	127 (6)	87 (8)	407 (18)		
	86 (7)	114 (8)	132 (7)	88 (9)	420 (20)		
C(9)	94 (6)	110 (6)	96 (6)	98 (8)	398 (18)		
	98 (7)	125 (7)	89 (7)	85 (8)	397 (20)		

Projection coefficient	R			$\Delta\beta_{11}$	$\Delta\beta_{22}$	$\Delta\beta_{13}$	$\Delta\beta_{33}$
	ωF^2	F^2	F				
140	220	87	95	−37 (20)	502 (49)	52 (8)	102 (7)
133	235	88	97	14 (59)	698 (145)	33 (13)	118 (22)

The uniformity of the gross populations in this structure contrasts with the results for more polar systems.

Roos & Skancke (1967) have predicted that second-order shifts should occur in structures of this type. An INDO calculation yielded gross Mulliken populations which are included in Fig. 4(*c*). The agreement between theory and experiment is poor, but this is expected, since it clearly arises from poor sampling of the density for the hydrogen atoms. The results for oxalic acid, after allowing for the lower displacement of the maximum-overlap position from the nuclear position in C–H bonds (Templeton, Olson, Zalkin & Templeton, 1970) suggest 0·10 e as a reasonable allowance for this effect. This brings the observed and theoretical values into agreement.

Diphenyl

It was not considered feasible to collect neutron diffraction data comparable in accuracy with Robertson's (1965) X-ray values, and it was decided that the analysis should stand on the X-ray data alone. 551 accurately measured Cu $K\alpha$ data were available. The defining vectors for the bond-directed scattering factors are given in Fig. 5(*a*). Population parameters and anisotropic temperature factors were determined for all atoms. The thermal ellipsoids for the hydrogen atoms, shown in Fig. 5(*b*) are all physically reasonable, in contrast with those obtained in the oxalate series. The population coefficients are given in Table 9. The values for chemically equivalent atoms agree within the error, and correspond qualitatively with the results of semi-empirical INDO calculations, shown in Fig. 5(*c*). The random error for the hydrogen populations is higher than for *p*-terphenyl, where the use of neutron thermal parameters gave higher precision, but there is no systematic downward bias since the density functions are now centred at the maximum overlap position.

The high quality of this data set offers the possibility of investigating the cusp condition. Stewart (1973*c*) has done this by the addition of a $1s2s$ orbital product, but the choice of this function is not unique, and in this case a $(1s)^2$ STO product was added at each carbon nucleus. Attempts at refining the exponent of this term were unsuccessful because of interaction with the thermal parameters, so this was fixed at the standard molecular *L*-shell value. The results are included in Table 9. The populations of the cusp term for the carbon atoms agree within the error. $\left(\frac{\partial \varrho}{\partial r}\Big/\varrho\right)_{r=0}$, which has the value of $-12{\cdot}028$ for the core, has a mean value of $-12{\cdot}004$ (3) when the extra term is included.

The data set was also used to check Stewart's (1972) conclusion that Fourier transforms of two-centre terms overlap so heavily with those of the adjacent one-centre products that separate inclusion is not warranted. To avoid a probable difficulty the antisymmetric one-centre ($2s2p$) functions, which contribute little to the density because of the uniformity of the in-plane pop-

Table 9. *Bond-directed scattering-factor refinements for diphenyl*

Bond-directed and total valence populations ($e \times 10^2$) rescaled to give a neutral molecule, with projection coefficient ($\times 10^2$) and refinement indices ($\times 10^3$). The vector directions associated with the scattering factors are given in Fig. 5(*a*).

	P_1	P_2	P_3	P_π	P_{cusp}	P_{val}		P_{val}
C(1)	93 (4)	83 (4)	84 (4)	124 (8)		383 (4)	H(2)	115 (5)
	85 (4)	79 (4)	79 (4)	123 (8)	21 (5)	388 (5)		122 (4)
C(2)	86 (5)	91 (5)	91 (5)	122 (12)		389 (4)	H(3)	108 (5)
	68 (5)	81 (5)	81 (5)	129 (12)	21 (8)	382 (5)		115 (4)
C(3)	97 (5)	98 (6)	98 (5)	103 (13)		397 (4)	H(4)	96 (5)
	76 (5)	83 (5)	84 (5)	109 (14)	31 (9)	385 (5)		99 (4)
C(4)	97 (5)	87 (5)	89 (5)	128 (11)		401 (4)	H(5)	103 (6)
	82 (5)	82 (5)	80 (5)	135 (11)	17 (8)	398 (3)		102 (4)
C(5)	86 (5)	89 (6)	91 (6)	130 (13)		391 (5)	H(6)	127 (6)
	81 (5)	82 (5)	90 (5)	127 (14)	16 (9)	393 (4)		140 (5)
C(6)	85 (5)	95 (5)	96 (5)	119 (12)		393 (4)		
	69 (4)	87 (5)	90 (5)	121 (12)	18 (8)	387 (3)		

Projection coefficient	R		
	ωF^2	F^2	F
84	139	85	35
95	133	80	34

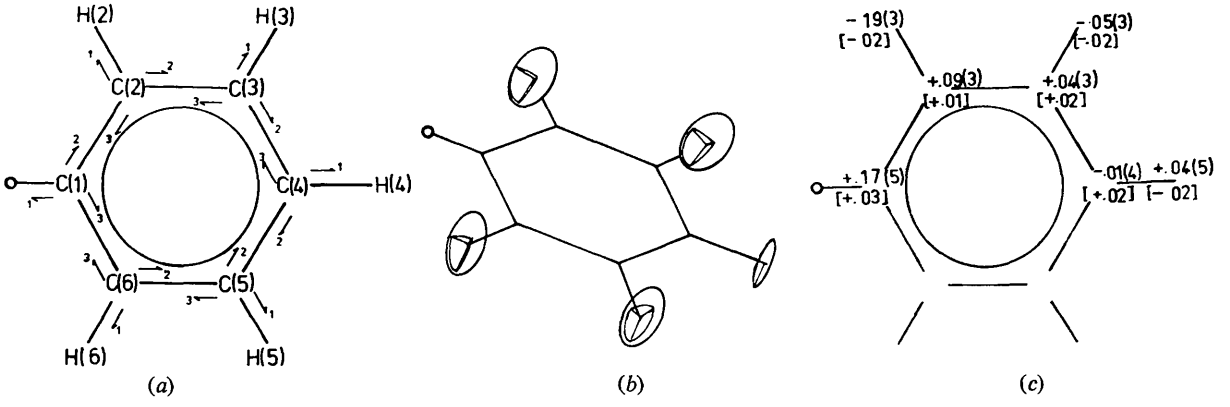

(*a*) (*b*) (*c*)

Fig. 5. Diphenyl – (*a*) atom numbering and directions for bond-directed scattering factors; (*b*) thermal ellipsoid r.m.s. amplitudes for the hydrogen atoms; (*c*) formal charges, with chemically equivalent values averaged and theoretical values in square brackets, Only the half molecule within the asymmetric unit of the structure is shown.

ulations, were excluded altogether, but for compatibility with the earlier refinements the remaining one-centre contributions were constructed from bond-directed $(p)^2$ orbital products. The two-centre term for each carbon–carbon bond A–B was represented as a sum of $2s_A2p_B$ and $2p_A2s_B$ contributions. The sum is a symmetric term which is close to a scalar function. The difference is a bond dipole term. Following an attempt to construct C–H two-centre functions from $2s_C1s_H$ and $2p_C1s_H$ contributions, which proved abortive because of high correlation, each two-centre C–H contribution was represented as a single $2s_C1s_H$ term. The radial dependence of the valence terms in this study were determined from SCF functions. Results for this analysis are given in Table 10. None of the bond dipole contributions differ appreciably from zero and the populations of the individual two-centre terms are uniformly small, and are negative with one exception. As a further check on the validity of this result the population parameters were redetermined using a mechanistic model for the thermal motion (Maslen, 1970). There was strong correlation between some of the parameters and the standard deviations increased, but the essential character of the populations remained unchanged.

Extension to second-row atoms

For a serious attempt at charge-density analysis on second-row atoms a set of extensive, high-quality data for a large structure containing one or two such atoms is required. Two sets seemed likely to prove satisfactory. Furberg & Jensen (1970) collected a set of 3774 Mo $K\alpha$ reflexions for thiocytosine. There are two molecules in the asymmetric unit of this structure, but it is non-centrosymmetric and intensities for Friedel pairs were not recorded separately. The cell also has a short b axis (4·0943 Å). A still more extensive data set (4365 Mo $K\alpha$ reflexions) was collected by Brown (1969) for 6-mercaptopurine monohydrate, which has a centrosymmetric structure. The low-angle reflexions for this set, denoted the OR data, were measured using an ω scan, taking particular care with the background estimation. The θ:2θ scan was employed for the high-angle data, and also for a second, apparently less accurate set, denoted the UW data, (1838 Mo $K\alpha$ reflexions) by Sletten, Sletten & Jensen (1969), using material of lower purity. There are systematic differences between these two sets, which are described by Brown (1969). The structure offers an opportunity for studying both the charge distribution of a sulphur atom and the effects of systematic experimental error on the analysis.

Thiocytosine

The charge-density model for the first-row atoms is similar to those for the earlier analyses. The density for the sulphur was represented as a neon-like core constructed from the SCF functions of Clementi (1965). After a model based on one $(sp^2)^2$ product directed along the S=C bond with two $(p)^2$ products normal to this had given rather poor sampling, the valence density was constructed in the same manner as for the ring atoms, except that M-shell STO functions were employed.

The defining vectors for the model and the results of the refinement are given in Fig. 6 and Table 11 respectively. The r.m.s. deviation between the gross populations for corresponding carbon and nitrogen atoms in the two molecules is a factor of two greater than the mean e.s.d. from the normal-equation matrix. This is some way short of ideal, but for hydrogen the r.m.s. deviation is more than four times larger than the calculated e.s.d.'s. Anomalously large populations for

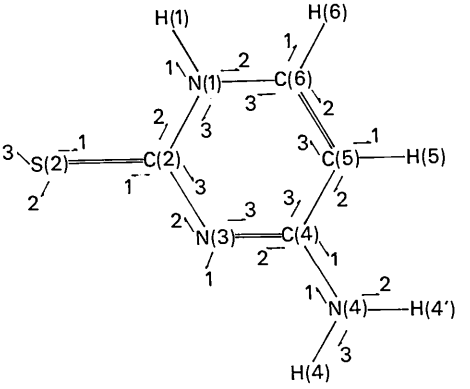

Fig. 6. Thiocytosine – atom numbering and directions for bond-directed scattering factors.

Table 10. *Valence-population refinements for diphenyl including two-centre terms*

Bond-directed, total one-centre valence and two-centre populations (e × 10^2) rescaled to give a neutral molecule, with projection coefficient (× 10^2) and refinement indices (× 10^3). The vector directions associated with the one-centre terms are given in Fig. 5(*a*).

	P_1	P_2	P_3	P_π	P_{val}		P_{val}
C(1)	50 (12)	38 (13)	42 (12)	75 (9)	405 (6)	H(2)	106 (5)
C(2)	34 (13)	45 (12)	41 (13)	83 (12)	403 (5)	H(3)	107 (5)
C(3)	37 (14)	47 (15)	39 (14)	82 (13)	405 (5)	H(4)	104 (5)
C(4)	39 (14)	43 (12)	39 (13)	83 (12)	404 (6)	H(5)	107 (5)
C(5)	34 (14)	40 (15)	44 (14)	87 (14)	405 (5)	H(6)	108 (8)
C(6)	31 (13)	39 (13)	53 (13)	80 (12)	403 (5)		

	P_{sp}	P_{ps}	P_{total}		P_{2s1s}
C(1)–C(2)	−2 (6)	−2 (6)	−4 (9)	C(2)–H(2)	−4 (4)
C(2)–C(3)	−1 (6)	−1 (6)	−2 (9)	C(3)–H(3)	−4 (4)
C(3)–C(4)	−3 (6)	−1 (6)	−4 (9)	C(4)–H(4)	−5 (4)
C(4)–C(5)	−1 (6)	−1 (6)	−2 (9)	C(5)–H(5)	−3 (4)
C(5)–C(6)	−3 (6)	+1 (6)	−2 (9)	C(6)–H(6)	−4 (4)
C(6)–C(1)	−1 (6)	−1 (6)	−2 (9)		
C(1)–C(1′)			−1 (3)		

Projection coefficient	*R*		
	ωF^2	F^2	F
98	161	128	46

H(5) in molecule *A* and H(4) and H(5) in molecule *B* are associated with improbably large amplitudes of thermal motion directed along the short *b* axis.

Although the thermal motions for the hydrogen atoms appear unreliable, those for the remaining atoms are well determined. A mechanistic model should predict the thermal motions of the hydrogen atoms with higher accuracy than those from direct least-squares refinement. The first stage in setting up such a model was the calculation of the rigid-body motions affecting the non-hydrogen atoms and motions of the sulphur and amino nitrogen relative to the ring proper (Varghese, 1974), following the general procedure of Johnson (1970*a*, *b*). Mean square amplitudes for the hydrogen atoms were calculated as the resultant of these motions, hindered rotation with an r.m.s. amplitude of 0·13 radians about the C–N bond to each amino group, in-plane and out-of-plane librations with r.m.s. amplitudes of 0·13 and 0·19 radians respectively, and a vibration with an r.m.s. amplitude of 0·08 Å along each X–H bond.

Population parameters calculated on this basis are included in Table 11. The consistency of the whole ensemble of populations is greatly improved. The agreement between the r.m.s. deviation and the e.s.d.'s for individual components is now comparable with that for the gross populations.

The charge distribution for the first-row atoms is as expected. The low P_π populations for the carbon atoms are consistent with those observed earlier. For the nitrogen atoms carrying negative charges the P_π populations are relatively higher. This is experimental verification of the fact that charge movements in systems of this type are associated primarily with the π electrons. The main disconcerting feature of the results is the low population for the sulphur atoms, which indicates that these are positively charged. Electronegativity considerations, and the position of the sulphur relative to C(2), N(1) and N(3) indicate that the sulphur atom should carry a negative charge. It thus appears that the basis functions sample the valence density less efficiently for this atom.

Table 11. *Bond-directed scattering-factor refinements for thiocytosine*

Bond-directed and total valence populations ($e \times 10^2$), dispersion terms ($e \times 10^3$) with projection coefficients ($\times 10^2$) and refinement indices ($\times 10^3$). The vector directions associated with the scattering factors are indicated in Fig. 6. The upper and lower results are those obtained using hydrogen parameters obtained directly from the refinement and from a mechanistic model respectively.

	Molecule	P_1	P_2	P_3	P_π	P_{val}	$\Delta f'$	$\Delta f''$
C(2)	*A*	86 (4)	97 (4)	99 (4)	79 (6)	360 (3)		
		95 (4)	100 (4)	98 (4)	76 (6)	370 (3)		
	B	116 (4)	109 (4)	96 (4)	77 (6)	398 (3)		
		125 (4)	87 (4)	103 (4)	83 (6)	398 (3)		
C(4)	*A*	102 (4)	93 (3)	100 (4)	63 (6)	358 (4)		
		91 (4)	94 (4)	110 (4)	70 (6)	365 (4)		
	B	94 (4)	108 (4)	114 (3)	97 (6)	413 (4)		
		85 (4)	93 (4)	112 (4)	92 (6)	383 (4)		
C(5)	*A*	79 (4)	99 (4)	123 (4)	67 (7)	368 (4)		
		84 (5)	109 (4)	118 (4)	90 (7)	400 (4)		
	B	81 (4)	133 (4)	135 (4)	54 (7)	402 (3)		
		107 (5)	129 (4)	121 (4)	64 (7)	422 (4)		
C(6)	*A*	114 (4)	110 (4)	109 (4)	70 (7)	404 (4)		
		99 (5)	113 (4)	93 (4)	81 (8)	387 (4)		
	B	100 (4)	121 (4)	118 (4)	71 (6)	410 (3)		
		104 (5)	104 (4)	108 (4)	87 (7)	404 (4)		
N(1)	*A*	98 (4)	140 (4)	130 (4)	141 (6)	509 (4)		
		109 (5)	129 (4)	129 (4)	145 (6)	511 (4)		
	B	117 (3)	126 (4)	149 (4)	135 (6)	526 (3)		
		119 (4)	119 (4)	132 (4)	152 (6)	535 (4)		
N(3)	*A*	133 (3)	125 (4)	131 (3)	111 (6)	500 (3)		
		129 (3)	126 (4)	131 (3)	122 (6)	508 (3)		
	B	145 (3)	145 (3)	144 (4)	116 (6)	550 (3)		
		153 (3)	147 (3)	131 (4)	119 (6)	550 (3)		
N(4)	*A*	132 (4)	107 (4)	133 (4)	137 (7)	508 (3)		
		120 (4)	110 (5)	129 (5)	142 (7)	501 (4)		
	B	136 (3)	108 (4)	122 (4)	140 (7)	505 (3)		
		122 (4)	110 (5)	129 (4)	145 (7)	506 (4)		
S(2)	*A*	159 (4)	135 (4)	132 (4)	146 (8)	572 (5)	53 (25)	−6 (16)
		157 (4)	119 (4)	126 (4)	134 (8)	535 (5)	71 (25)	−3 (16)
	B	146 (4)	130 (5)	126 (4)	159 (8)	561 (6)	49 (24)	13 (19)
		158 (4)	151 (5)	130 (4)	171 (8)	610 (6)	−9 (24)	51 (19)

	Molecule	P_{val}
H(1)	*A*	111 (4)
		116 (5)
	B	94 (4)
		94 (4)
H(4)	*A*	59 (3)
		89 (4)
	B	84 (4)
		85 (4)
H(4′)	*A*	102 (4)
		89 (4)
	B	84 (4)
		87 (4)
H(5)	*A*	148 (4)
		127 (4)
	B	141 (4)
		108 (4)
H(6)	*A*	114 (3)
		129 (4)
	B	119 (4)
		104 (4)

Projection coefficient	*R*		
	ωF^2	F^2	F
96	67	39	31
95	66	37	31

6-Mercaptopurine monohydrate

Initially the OR data were analysed using a density model similar to that for thiocytosine, but convergence was slow and thermal parameters for four of the hydrogen atoms became non-positive definite. To eliminate interaction between the atom shapes and the thermal parameters the refinement was carried out at the gross population level. The UW data was analysed in parallel at the same level. Convergence with the OR data remained slow, and the hydrogen populations were correlated with the thermal parameters as in the ammonium oxamate analysis. The projection coefficients and refinement indices are given in Table 12, and the formal charges are given in Fig. 7.

Table 12. *Projection coefficients and refinement indices for 6-mercaptopurine monohydrate*

The upper and lower values correspond to the OR and UW data respectively.

Projection coefficient ($\times 10^2$)	$R(\times 10^3)$ ωF^2	F^2	F
88	119	87	90
100	106	53	44

The distribution of charge for the OR data is unsatisfactory. Both C(4) and C(5) carry large negative charges, although it is obvious from its proximity to two nitrogens that C(4) at least should be positively charged. For the UW data, on the other hand, the results, apart from a low population for N(1) are consistent with those for thiocytosine. The low population for the sulphur atom is confirmed. H(2) carries a negative charge, which follows a general tendency of the charge to alternate in this part of the structure. It has been postulated, on the basis of the intermolecular geometry that H(2) is involved in a C–H···N hydrogen bond (Sletten, Sletten & Jensen, 1960). While this might be true for a negatively charged carbon such as that at the 5 position in uracil (Stewart, 1970) it is highly improbable in this structure.

Intensity measurement and charge density

In single-crystal projects (McKenzie & Maslen, 1968; Abrahams, Hamilton & Mathieson, 1970; Hamilton & Abrahams, 1970) it has been found that the ω-scan method produces outliers in the intensity measurements. The results from the OR data for 6-mercaptopurine monohydrate suggest that these outliers are in fact errors. They also indicate that a systematic bias with Bragg angle in the low-angle data will produce gross discrepancies in the charge density.

An experimental technique which is known to produce a bias in the data is the stationary-crystal/stationary-counter method, which is similar in many respects to an ω scan in which no special precautions are taken in estimating the background. Fortunately two sets of data on related materials were collected at about the same time in the same laboratory, using different scanning techniques.

Data for *N*-methyl-*N*,2,4,6 tetranitroaniline (Tetryl), collected by Cady (1967), consist of 1808 reflexions measured with Mo $K\alpha$ radiation using the stationary-crystal/stationary-counter method. Gross charges determined for these data are illustrated in Fig. 8(*a*), along with those from an INDO calculation. The disagreement is obvious. The variation of the ratio of the ob-

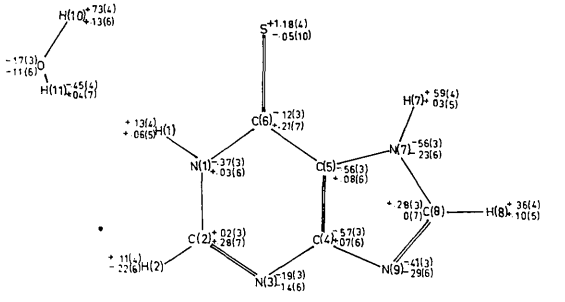

Fig. 7. 6-Mercaptopurine monohydrate – atom numbering and net charges. The upper and lower figures are derived from the OR and UW data respectively.

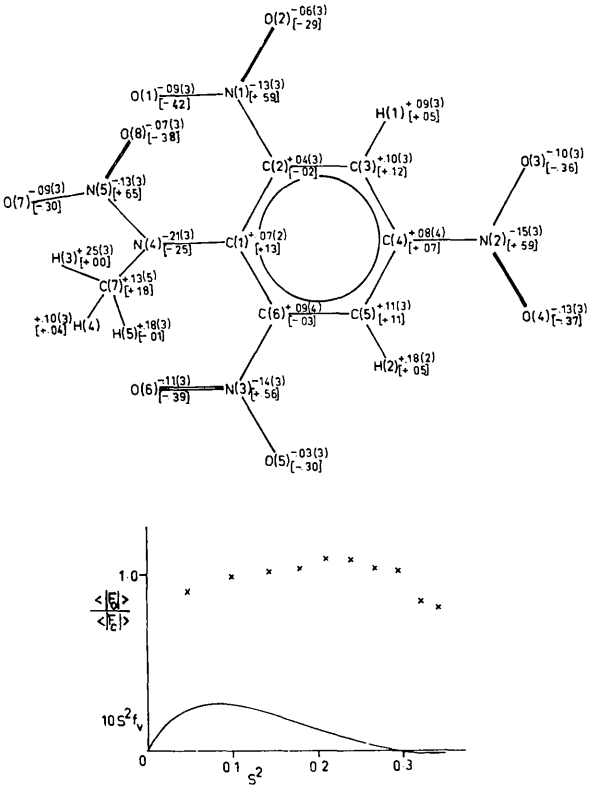

Fig. 8. *N*-Methyl-*N*,2,4,6 tetranitroaniline (Tetryl) – (*a*) atom numbering and net charges, with theoretical values in square brackets (*b*) variation of $\langle|F_o|\rangle/\langle|F_c|\rangle$ as functions of S^2. The solid line is the function f_vS^2, where f_v is the valence scattering factor for nitrogen. ($S=\sin\theta/\lambda$).

served to calculated structure amplitude as a function of Bragg angle for this data is shown in Fig. 8(*b*). There is clearly a bias in the data, which spuriously enhances the nitrogen populations.

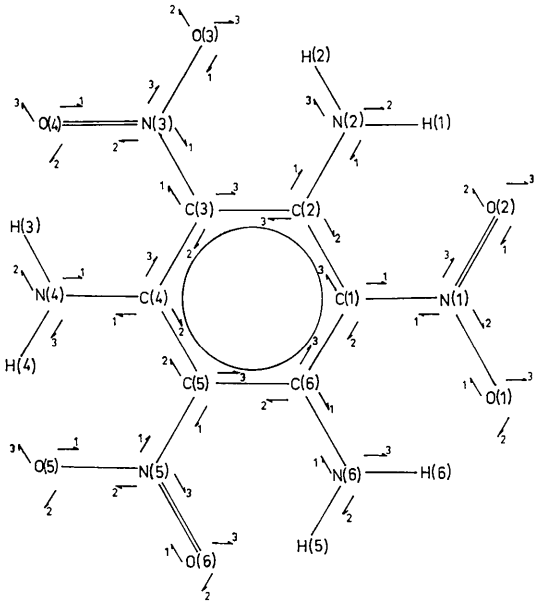

Fig. 9. *sym*-Triamino-trintrobenzene – atom numbering and directions for bond-directed scattering factors.

sym-Triamino-trinitrobenzene

A more limited set of data (927 Mo $K\alpha$ reflexions) was collected for *sym*-triamino-trinitrobenzene (Cady & Larson, 1965) by the θ:2θ method. An agreement analysis on this data shows no evidence for systematic errors. The structure is an attractive one for charge-density analysis because the carbon and nitrogen atoms in the molecule are equivalent in threes, and the hydrogen and oxygen atoms in sixes. These atoms are crystallographically independent, which has been exploited by O'Connell, Rae & Maslen (1966) in a study of bonding *via* the difference density.

Preliminary results were encouraging and the charge-density model was extended to include bond-directed scattering factors. These were directed as in Fig. 9, and the results of the analysis are shown, along with gross Mulliken populations from an INDO calculation, in Table 13.

The calculated e.s.d.'s for the gross populations for the carbon, nitrogen and oxygen atoms agree with error estimates based on the internal consistency of the results. For individual components the calculated e.s.d.'s are 20% too low, and for the hydrogen populations they are 90% too low. There is a rapid increase in the size of these e.s.d.'s of the π components of the density with distance from the ring centre, which corresponds to increased thermal motion. Thus although the e.s.d.'s for the gross populations of oxygen and carbon are comparable they differ in the ratio of 3:1 for the P_π populations.

Table 13. *Bond-directed scattering-factor refinements for sym-triamino-trinitrobenzene*

Bond-directed and total valence populations ($e \times 10^2$) with projection coefficients ($\times 10^2$) and refinement indices ($\times 10^3$). In each case P_1 is the unique population, directed axially for the carbon and nitrogen atoms, and towards the nitrogen for the oxygen atoms. P_{theor} is the gross Mulliken population from an INDO calculation.

	P_1	P_2	P_3	P_π	P_{val}	P_{theor}
C(1)	67 (12)	86 (12)	83 (12)	162 (25)	397 (9)	421
C(3)	53 (11)	57 (11)	63 (12)	220 (25)	394 (9)	424
C(5)	77 (12)	91 (12)	81 (13)	163 (26)	411 (9)	421
C(2)	81 (11)	78 (12)	78 (12)	143 (25)	379 (9)	368
C(4)	77 (12)	89 (12)	89 (12)	126 (27)	381 (9)	368
C(6)	67 (12)	70 (12)	76 (12)	171 (25)	385 (9)	368
N(1)	83 (14)	84 (14)	82 (15)	240 (24)	489 (8)	440
N(3)	89 (15)	76 (14)	96 (15)	227 (36)	489 (8)	437
N(5)	136 (14)	119 (13)	124 (14)	118 (34)	497 (8)	440
N(2)	91 (14)	79 (16)	77 (14)	266 (36)	513 (8)	522
N(4)	106 (16)	93 (14)	89 (15)	227 (36)	515 (8)	524
N(6)	118 (14)	104 (15)	101 (16)	196 (36)	519 (8)	523
O(1)	138 (21)	142 (22)	131 (20)	211 (57)	623 (9)	641
O(2)	128 (20)	127 (19)	128 (19)	244 (51)	627 (9)	643
O(3)	128 (23)	98 (23)	124 (22)	279 (60)	630 (9)	642
O(4)	157 (18)	157 (20)	148 (19)	146 (51)	608 (9)	641
O(5)	165 (19)	158 (20)	155 (20)	136 (21)	614 (9)	643
O(6)	167 (18)	174 (18)	174 (17)	104 (47)	618 (9)	641
H(1)					82 (8)	82
H(2)					78 (9)	83
H(3)					105 (11)	82
H(4)					79 (11)	82
H(5)					105 (11)	82
H(6)					62 (11)	83

Projection coefficient	R		
	ωF^2	F^2	F
92	126	72	56
92	85	67	52

Although the experimental gross populations agree only qualitatively with the theoretical values there is no bias with atom type, and hence no evidence for systematic error. The discrepancy is primarily a difference in the degree of polarity of the C–N linkages with the nitro groups. This appears to indicate a limitation in the accuracy of the semi-empirical calculations. The method of comparison itself involves some approximations. Ideally the theoretical density should be projected onto the basis functions used in the experimental analysis. A suitable procedure is described by Newton (1969) but it is rather time consuming, and would certainly not produce changes of the size necessary to bring the INDO result into accord with the experimental values. It would be justified only in comparing accurate theoretical calculations with precise experimental results.

A further refinement was carried out using two-centre terms similar to those described above for diphenyl, the only difference being that the N–H terms were constructed from $2s_N$–$1s_H$ and $2p_N$–$1s_H$ products instead of a single product. The results of this refinement are given in Table 14. There is consistency, not only in the sums of the populations, which correspond roughly to bond charges, but also in the differences, which are bond dipole terms. The bond charges are uniformly close to zero, as in diphenyl. For the C–N linkages there has been some interaction between the bond dipoles and the scalar populations, but the latter are further removed from the theoretical values. The inclusion of two-centre terms in this form does not appear to be a profitable method for exploring charge densities.

Conclusion

In favourable cases charge-density analyses using kinematic diffraction data have yielded results which can be compared with theoretical calculations for molecular crystals containing the lighter atoms. The favourable cases do not include structures with small cell dimensions, for which poor sampling in the low-angle region of reciprocal space limits the precision which may be achieved.

Gross populations are insensitive to deficiencies in the thermal model, and to residual errors in thermal parameters for extensive data sets, except for hydrogen. Simultaneous determination of gross charge and thermal motion for hydrogen taxes the data, and is a good test of quality. Analysis of the shape of the electron distribution is more sensitive to deficiencies in the thermal model, and the precision which can be achieved falls off rapidly with increased thermal motion.

A spherically symmetric form factor for bonded hydrogen does not overlap efficiently with the observed density if it is centred at the nuclear position. Coppens (1972) has recently shown that the inclusion of a simple *sp* dipole term does not solve the problem completely. Coulson & Thomas (1971) and Thomas (1971, 1972) have shown that when an asymmetric distribution oscillates harmonically the peak of the distribution is displaced, but this does not account for the discre-

Table 14. *Valence-population refinement for sym-triamino-trinitrobenzene including two-centre terms*

Bond-directed $(p)^2$ total one-centre valence and two-centre populations ($e \times 10^2$) rescaled to give a neutral molecule, with projection coefficient ($\times 10^2$) and refinement indices ($\times 10^3$). The vector directions associated with the one-centre terms are given in Fig. 9.

	P_1	P_2	P_3	P_π	P_{val}
C(1)	6 (24)	47 (23)	21 (22)	106 (22)	395 (9)
C(3)	23 (23)	−28 (24)	60 (24)	137 (22)	406 (9)
C(5)	54 (23)	53 (22)	−13 (23)	107 (22)	416 (9)
C(2)	30 (23)	25 (22)	−3 (23)	109 (21)	377 (9)
C(4)	−5 (23)	48 (22)	4 (23)	96 (22)	358 (9)
C(6)	24 (22)	13 (24)	6 (24)	126 (22)	384 (9)
N(1)	59 (30)	69 (30)	57 (30)	113 (31)	513 (14)
N(3)	99 (31)	32 (30)	15 (32)	167 (32)	527 (13)
N(5)	68 (31)	81 (31)	36 (31)	118 (31)	517 (8)
N(2)	92 (29)	3 (30)	51 (29)	162 (31)	522 (8)
N(4)	11 (31)	93 (30)	42 (31)	172 (32)	532 (11)
N(6)	33 (31)	81 (30)	50 (30)	157 (31)	536 (8)
O(1)	−33 (45)	85 (44)	56 (43)	270 (50)	593 (9)
O(2)	−8 (44)	65 (44)	100 (41)	241 (47)	614 (8)
O(3)	−78 (48)	13 (46)	148 (40)	306 (53)	604 (9)
O(4)	14 (41)	43 (43)	76 (40)	243 (45)	591 (8)
O(5)	−31 (45)	56 (43)	54 (47)	295 (45)	589 (8)
O(6)	−71 (43)	148 (38)	135 (39)	179 (45)	606 (8)
H(1)	77 (8)				
H(2)	74 (9)				
H(3)	84 (9)				
H(4)	84 (10)				
H(5)	77 (9)				
H(6)	66 (11)				

	P_{sA-sB}	P_{sA-pB}	P_{pA-sB}	P_{bond}
C(1)–C(2)		−8 (10)	17 (10)	9 (6)
C(3)–C(2)		−6 (10)	9 (10)	3 (6)
C(3)–C(4)		0 (9)	8 (10)	8 (6)
C(5)–C(4)		12 (9)	−5 (10)	7 (6)
C(5)–C(6)		11 (9)	−6 (9)	5 (6)
C(1)–C(6)		18 (10)	−4 (10)	13 (6)
C(1)–N(1)		−16 (14)	14 (12)	−2 (8)
C(3)–N(3)		−12 (14)	17 (12)	5 (8)
C(5)–N(5)		−8 (14)	13 (12)	5 (8)
C(2)–N(2)		11 (10)	−11 (9)	0 (6)
C(4)–N(4)		11 (11)	−7 (10)	4 (6)
C(6)–N(6)		7 (9)	−9 (13)	−2 (7)
N(1)–O(1)		43 (9)	−41 (14)	2 (8)
N(1)–O(2)		26 (9)	−34 (14)	−7 (8)
N(3)–O(3)		50 (10)	−59 (14)	−6 (9)
N(3)–O(4)		33 (9)	−39 (13)	−6 (8)
N(5)–O(5)		43 (10)	−38 (14)	5 (7)
N(5)–O(6)		30 (10)	−30 (14)	−1 (8)
N(2)–H(1)	33 (17)	−24 (11)		8 (8)
N(2)–H(2)	41 (18)	−36 (12)		5 (9)
N(4)–H(3)	17 (26)	−15 (17)		2 (13)
N(4)–H(4)	48 (25)	−47 (16)		1 (12)
N(6)–H(5)	38 (19)	−34 (13)		5 (10)
N(6)–H(6)	17 (18)	−23 (12)		−6 (9)

Projection coefficient	R		
	ωF^2	F^2	F
93	116	61	49

pancy. The apparent shortening of an X–H bond due to bonding-electron asymmetry is increased if a spherically averaged form factor is used in the analysis, but if the form factor had the correct asymmetric form the thermal motion would be correctly deconvoluted, and there would be no such displacement. Development of improved form factors for hydrogen is necessary if accurate bond lengths and populations are to be determined.

This work has been supported financially by the Australian Research Grants Committee, by the Australian Institute of Nuclear Science and Engineering, and by the Research Committee of the University of Western Australia. Their assistance is gratefully acknowledge. The authors are indebted to G. M. Brown, H. H. Cady, L. H. Jensen, A. C. Larson and G. B. Robertson for providing detailed intensity data, and to R. F. Stewart for helpful advice and assistance.

References

ABRAHAMS, S. C., HAMILTON, W. C. & MATHIESON, A. MCL. (1970). *Acta Cryst.* A**26**, 1–18.
BEAGLEY, B. & SMALL, R. W. H. (1963). *Proc. Roy. Soc.* A**275**, 469–491.
BEAGLEY, B. & SMALL, R. W. H. (1964). *Acta Cryst.* **17**, 783–788.
BENTLEY, J. & STEWART, R. F. (1974). *Acta Cryst.* A**30**, 60–67.
BRACHER, B. H. & SMALL, R. W. H. (1970). *Acta Cryst.* B**26**, 1705–1709.
BROWN, G. M. (1969). *Acta Cryst.* B**25**, 1338–1353.
CADY, H. H. (1967). *Acta Cryst.* **23**, 601–609.
CADY, H. H. & LARSON, A. C. (1965). *Acta Cryst.* **18**, 485–496.
CLEMENTI, E. (1965). *IBM J. Res. Dev. Suppl.* 9.
CLEMENTI, E. (1967). *J. Chem. Phys.* **46**, 4731–4742.
COPPENS, P. (1972). *Acta Cryst.* B**28**, 1638–1640.
COPPENS, P., CSONKA, L. & WILLOUGHBY, T. V. (1970). *Science*, **167**, 1126–1128.
COPPENS, P., PAUTLER, D. & GRIFFIN, J. F. (1971). *J. Amer. Chem. Soc.* **93**, 1051–1058.
COULSON, C. A. (1961). *Valence*, 2nd ed. Oxford Univ. Press.
COULSON, C. A. & THOMAS, M. W. (1971). *Acta Cryst.* B**27**, 1354–1359.
DAWSON, B. (1967*a*). *Proc. Roy. Soc.* A**298**, 255–263.
DAWSON, B. (1967*b*). *Proc. Roy. Soc.* A**298**, 264–288.
DELAPLANE, R. G. & IBERS, J. A. (1969). *Acta Cryst.* B**25**, 2423–2437.
EPSTEIN, J. (1972). B. Sc. Honours Thesis, Univ. of Western Australia.
FURBERG, S. & JENSEN, L. H. (1970). *Acta Cryst.* B**26**, 1260–1268.
FURINA, R. & MASLEN, E. N. (1975). To be published.
GRANT, D. F., KILLEAN, R. C. G. & LAWRENCE, J. L. (1969). *Acta Cryst.* B**25**, 377–379.
HAMILTON, W. C. & ABRAHAMS, S. C. (1970). *Acta Cryst.* A**26**, 19–24.
HEHRE, W. J., STEWART, R. F. & POPLE, J. A. (1969). *J. Chem. Phys.* **51**, 2657–2664.
HODGSON, D. J. & IBERS, J. A. (1969). *Acta Cryst.* B**25**, 469–477.
International Tables for Crystallography (1962). Vol. III. Birmingham: Kynoch Press.
JOHNSON, C. K. (1970*a*). *Thermal Neutron Diffraction*, Edited by B. T. M. WILLIS, pp. 132–160. Oxford Univ. Press.
JOHNSON, C. K. (1970*b*). *Crystallographic Computing*, Edited by F. R. AHMED, pp. 207–219. Copenhagen: Munksgaard.
KILLEAN, R. C. G. & LAWRENCE, J. L. (1969). *Acta Cryst.* B**25**, 1750–1752.
KILLEAN, R. C. G., LAWRENCE, J. L. & SHARMA, V. C. (1972). *Acta Cryst.* A**28**, 405–407.
LIPSCOMB, W. N. (1972). *Trans. Amer. Cryst. Assoc.* **8**, 79–88.
MCDONALD, T. R. R. (1960). *Acta Cryst.* **13**, 113–124.
MCKENZIE, J. K. & MASLEN, V. W. (1968). *Acta Cryst.* A**24**, 628–639.
MCWEENY, R. (1952). *Acta Cryst.* **5**, 463–468.
MCWEENY, R. (1954). *Acta Cryst.* **7**, 180–186.
MASLEN, E. N. (1970). *Crystallographic Computing*, Edited by F. R. AHMED, pp. 231–242. Copenhagen: Munksgaard.
MEULENAER, J. DE & TOMPA, H. (1965). *Acta Cryst.* **19**, 1014–1018.
NEWTON, M. D. (1969). *J. Chem. Phys.* **51**, 3917–3926.
O'CONNELL, A. M., RAE, A. I. M. & MASLEN, E. N. (1966). *Acta Cryst.* **21**, 208–219.
O'CONNOR, B. H. & MASLEN, E. N. (1974). *Acta Cryst.* B**30**, 383–389.
PERSSON, E. & GRIMVALL, G. (1970). *Acta Cryst.* A**26**, 519–522.
POPLE, J. A. & BEVERIDGE, D. L. (1972). *Approximate Molecular Orbital Theory*. New York: McGraw-Hill.
RIETVELD, H. M., MASLEN, E. N. & CLEWS, C. J. B. (1970). *Acta Cryst.* B**26**, 693–706.
ROBERTSON, G. B. (1965). Ph. D. Thesis, Univ. of Western Australia.
ROOF, R. B. JR, (1967). American Crystallographic Association Winter Meeting, Atlanta, Georgia. Abstract A2.
ROOS, B. & SKANCKE, P. N. (1967). *Acta Chem. Scand.* **21**, 233–242.
SABINE, T. M., COX, G. W. & CRAVEN, B. M. (1969). *Acta Cryst.* B**25**, 2437–2441.
SEQUEIRA, A., SRIKANTA, S. & CHIDAMBARAM, R. (1970). *Acta Cryst.* B**26**, 77–82.
SLETTEN, E., SLETTEN, J. & JENSEN, L. H. (1969). *Acta Cryst.* B**25**, 1330–1338.
STEWART, R. F. (1969). *J. Chem. Phys.* **51**, 4569–4577.
STEWART, R. F. (1970). *J. Chem. Phys.* **53**, 205–213.
STEWART, R. F. (1972). *Acta Cryst.* A**28**, S7.
STEWART, R. F. (1973*a*). Private communication.
STEWART, R. F. (1973*b*). *J. Chem. Phys.* **58**, 4430–4438.
STEWART, R. F. (1973*c*). *Acta Cryst.* A**29**, 602–605.
TEMPLETON, D. H., OLSON, A. J., ZALKIN, A. & TEMPLETON, L. K. (1972). *Acta Cryst.* A**28**, S252.
THOMAS, M. W. (1971). *Acta Cryst.* B**27**, 1760–1765.
THOMAS, M. W. (1972). *Acta Cryst.* B**28**, 2206–2212.
VARGHESE, J. N. (1974). Ph. D. Thesis, Univ. of Western Australia.
ZACHARIASEN, W. (1967). *Acta Cryst.* **23**, 558–564.